JOURNAL OF VIROLOGY, Feb. 2006, p. 1204–1213 Vol. 80, No. 3
0022-538X/06/$08.00+0 doi:10.1128/JVI.80.3.1204–1213.2006

Paramyxovirus Receptor-Binding Molecules: Engagement of One Site on the Hemagglutinin-Neuraminidase Protein Modulates Activity at the Second Site

Matteo Porotto,[1] Micaela Fornabaio,[2] Olga Greengard,[3] Matthew T. Murrell,[4] Glen E. Kellogg,[2] and Anne Moscona[1]*

Departments of Pediatrics and of Microbiology and Immunology, Weill Medical College of Cornell University, 515 East 71st St., Box 309, New York, New York 10021,[1] Department of Medicinal Chemistry & Institute for Structural Biology and Drug Discovery, Box 980540, Virginia Commonwealth University, Richmond, Virginia 23298,[2] Mount Sinai School of Medicine, Department of Pediatrics, New York, New York 10029,[3] and Mount Sinai School of Medicine, New York, New York 10029[4]

Received 19 August 2005/Accepted 4 November 2005

The hemagglutinin-neuraminidase (HN) protein of paramyxoviruses carries out three different activities: receptor binding, receptor cleaving (neuraminidase), and triggering of the fusion protein. These three discrete properties each affect the ability of HN to promote viral fusion and entry. For human parainfluenza type 3, one bifunctional site on HN can carry out both binding and neuraminidase, and the receptor mimic, zanamivir, impairs viral entry by blocking receptor binding. We report here that for Newcastle disease virus, the HN receptor avidity is increased by zanamivir, due to activation of a second site that has higher receptor avidity. Only certain receptor mimics effectively activate the second site (site II) via occupation of site I; yet without activation of this second site, binding is mediated entirely by site I. Computational modeling designed to complement the experimental approaches suggests that the potential for small molecule receptor mimics to activate site II, upon binding to site I, directly correlates with their predicted strengths of interaction with site I. Taken together, the experimental and computational data show that the molecules with the strongest interactions with site I—zanamivir and BCX 2798—lead to the activation of site II. The finding that site II, once activated, shows higher avidity for receptor than site I, suggests paradigms for further elucidating the regulation of HN′s multiple functions in the viral life cycle.

Paramyxoviruses, including human parainfluenza virus type 3 (HPIV3) and the avian paramyxovirus Newcastle disease virus (NDV), possess an envelope protein hemagglutinin-neuraminidase (HN) that has receptor-cleaving as well as receptor-binding activity. HN is also essential for activating the fusion protein (F) to mediate the merger of the viral envelope with the host cell membrane. For both HPIV3 and NDV, this one molecule carries out three different but critical activities at specific points in the process of viral entry, and understanding the regulation of these activities is key for the design of strategies that block viral entry (19).

We have previously used a small molecule receptor mimic, zanamivir (4-guanidino-neu5Ac2en [DANA]), to probe paramyxovirus active sites and found distinctions between HPIV3 HN and NDV HN that are manifested by differences in the sensitivity of individual HN functions to zanamivir. Zanamivir can reversibly occupy the neuraminidase active site/receptor-binding site of HPIV3 HN (17). The compound was originally developed as an influenza neuraminidase inhibitor and has a sialidase K_i (M) of approximately 1×10^{-9} for the influenza A neuraminidase (13). The K_i for the parainfluenza virus neuraminidases is lower, approximately 8×10^{-4} for HPIV2, the virus for which values have been obtained (13).

For HPIV3, zanamivir inhibited both the receptor-binding function and the neuraminidase function of HN (12) but had its primary anti-infective effect by blocking receptor binding and thus impairing entry. A mutation at the active site (T193I for HPIV3) that substituted a bulky isoleucine for the threonine led to decreased affinity of zanamivir for the active site of the mutated HN (24). Structural analysis suggested that steric hindrance accounts for the reduced binding of zanamivir to HPIV3 HN, by excluding zanamivir from the binding pocket, and thus accounts for resistance to the compound of both receptor-binding and neuraminidase activities (24). These data suggested that the T193 active site on the HN of HPIV3 is bifunctional.

Crystallographic studies of the NDV HN (8, 28) and the HPIV3 HN (17) indicated that a single active site on the globular head of the molecule can indeed provide both receptor-binding and neuraminidase activities. For NDV, mutations in this site, site I, may alter receptor binding (5, 18), providing experimental evidence for the importance of this site to receptor binding. However, the effect of zanamivir on NDV HN (B1, an attenuated strain) is different from that on HPIV3: the NDV B1 HN receptor-binding function is strikingly resistant to the effect of zanamivir, while its neuraminidase activity is as sensitive to inhibitor as that of HPIV3 (24). The anti-infective effect of zanamivir on NDV (for the B1 strain) is therefore due to a failure of progeny virion release resulting from this neuraminidase inhibition (20, 24). The finding that NDV's receptor binding was resistant to zanamivir while its neuraminidase was sensitive (24) was consistent with the presence of two active

* Corresponding author. Mailing address: Departments of Pediatrics and of Microbiology and Immunology, Weill Medical College of Cornell University, 515 East 71st St., Box 309, New York, NY 10021. Phone: (212) 746-4801. Fax: (212) 746-8261. E-mail: anm2047@med.cornell.edu.

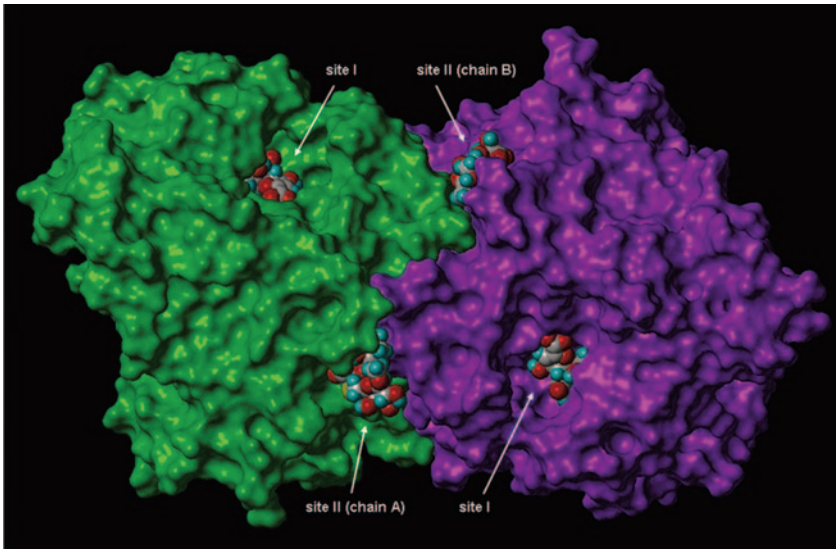

FIG. 1. NDV HN dimer crystal structure (from reference 28). The surface rendering was created with MOLCAD (Tripos, Inc., St. Louis, MO). The two chains, arising from the two HN monomers, are termed A and B. Chain A is shown in green, and chain B is shown in violet. The two binding sites for each chain are indicated. Each site is bound with the following crystallographically determined ligands: DANA at both sites I, thiosialoside at site II for chain A, and sialic acid at site II for chain B.

sites on NDV HN, one exhibiting both neuraminidase and receptor-binding activity and the second, only receptor binding. The first, site I, with both enzymatic activity and the receptor-binding function, can be inhibited by zanamivir, while site II possesses the receptor-binding function only and is insensitive to zanamivir (20).

The three-dimensional structure of the NDV HN (8) indeed revealed that, in addition to the primary active site which can carry out both binding and neuraminidase activities, the molecule also contains a second putative HN receptor-binding site in the groove of the dimer interface between two NDV-HN molecules (28). Figure 1 illustrates the two binding sites as seen in the NDV HN dimer crystal structure reported by Zaitsev et al. (28). It is important to note that both site I and site II are only partially occluded and the bound ligands at these sites are quite accessible to solvent or for exchange. The arginine at position 516 is an important residue in this binding pocket; mutations at this position affect fusion promotion and viral entry, suggesting that this second binding site on NDV-HN contributes to these functions (3).

In the present study, we investigated the operation of the NDV HN site II and its functional relationship to the bifunctional site I. In order to differentiate the functions that reside in each of the two sites, wild type (WT) NDV HN (AV; Australia-Victoria) and several small molecule receptor analogs (zanamivir, I; DANA, II; 2,3-sialyllactose, III; 2,6-sialyllactose, IV) were used as tools for probing the receptor-binding and neuraminidase functions of NDV HN. (See Fig. 2 for structures of the compounds discussed in this paper.) In parallel, we carried out a molecular modeling study where these compounds and others (thiosialoside, V; sialic acid, VI; BCX 2798, VII), when not already present in the crystal structures, were docked into these two active sites by using structural data (see Materials and Methods), and their relative binding energies were calculated.

The compound BCX 2798 (4-azido-5-isobutyrylamino-2,3-didehydro-2,3,4,5-tetradeoxy-D-glycero-D-galacto-2-nonulopyranosic acid, VII) was developed through structure-based drug design based on the structure of DANA bound to the active site of the NDV HN (2). This molecule differs from DANA in that the O4 hydroxyl group has been replaced with an azido group designed to more completely fill the active site cavity and the C5 methyl has been replaced with isopropyl. The compound has obvious structural similarity to zanamivir; however, its particular interest to our modeling study lay in the finding that, while BCX 2798 showed no inhibition of WT NDV HN binding, binding of an R516A mutant HN could be inhibited by the compound (3). This finding suggested that perhaps BCX 2798, like zanamivir, could bind to site I and activate site II. For HPIV3 on the other hand, BCX 2798 was shown to inhibit HPIV3 HN′s receptor binding (2). In fact, this compound was effective in reducing HPIV infection in mice (1, 2).

Experimental observations from our laboratory (20, 23, 24) and observations from other laboratories (2, 3, 6) appeared to be consistent with a single mechanism: molecules that effectively interact with NDV HN′s site I can activate site II and promote continued receptor binding, while interaction of the same molecules with HPIV3 HN′s bifunctional receptor-binding site prevents receptor binding. The qualitative agreement between the experimental and modeling results described in this paper are support for such a unique mechanism, wherein engagement of NDV HN′s primary binding site modulates activity at the other binding site. We suggest that, when structural information is available, in silico studies coordinated with detailed experimental measurements produce a powerful roadmap for understanding the structure and activities of paramyxovirus HN molecules.

MATERIALS AND METHODS

Cells. 293T (human kidney epithelial) cells were grown in Dulbecco's modification of Eagle's medium (Mediatech Cellgro) supplemented with 10% fetal

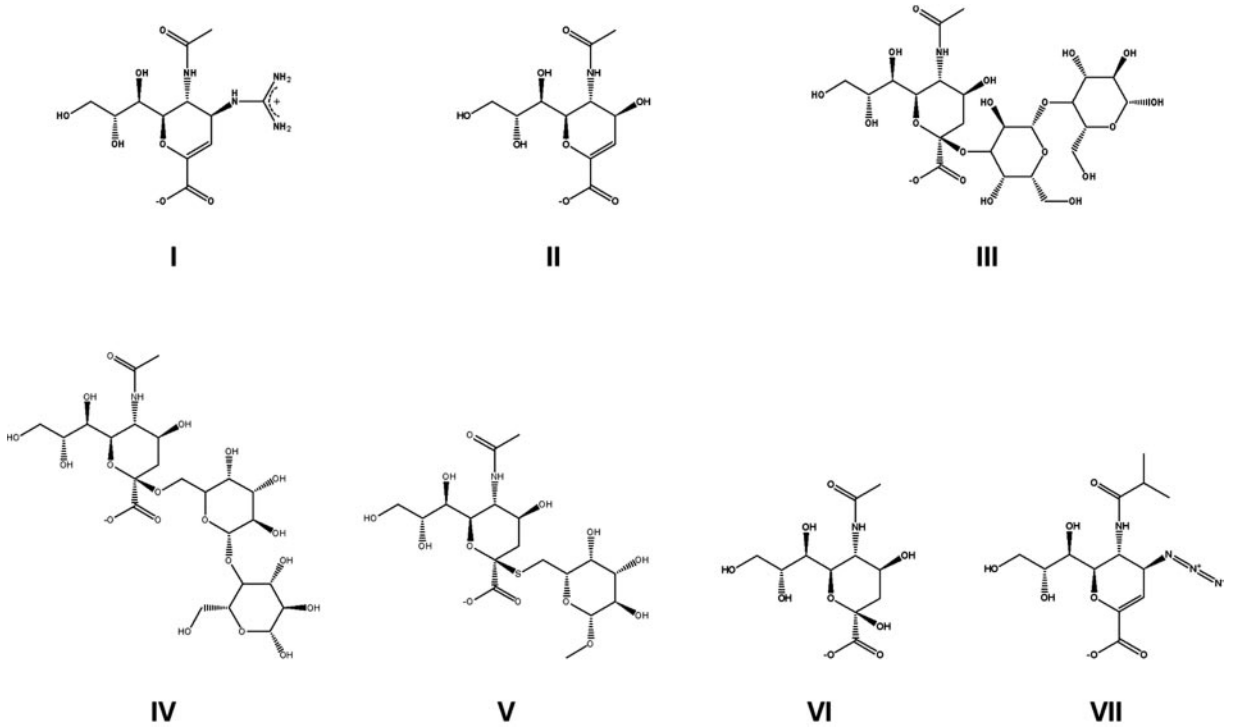

FIG. 2. Chemical structures of the compounds in this study. The interactions of these compounds with the two NDV active sites (I and II) have been analyzed experimentally and computationally.

bovine serum and antibiotics. For assays of cells in air at different pHs, the above medium was replaced with a CO_2-independent medium (Invitrogen) which was adjusted following the manufacturer's instructions to the indicated pH (21).

Chemicals. 4-Guanadino-DANA (zanamivir) (I) was prepared from Relenza Rotadisks (5 mg zanamivir with lactose). A 50 mM stock solution was prepared by dissolving each 5-mg blister capsule in 285 μl serum-free medium. Stock solutions were stored at −20°C. 2,3- and 2,6-sialyllactose (III, IV) and DANA (II) were obtained from Sigma Chemical Company (St. Louis, MO).

HN and F constructs. Mutagenized HPIV3 HN cDNAs were digested with SacI and BamHI and ligated into digested pCAGGS mammalian expression vectors as previously described (20). NDV AV WT HN in pCAGGS was obtained from Ronald Iorio.

Transient expression of HN and F genes. Transfections were performed according to the Lipofectamine Plus manufacturer's protocols (Invitrogen).

Quantification of cell surface expression of HN by ELISA. To quantify the amount of HN expressed on the cell surface of 293T cells, an enzyme-linked immunosorbent assay (ELISA) was performed as described previously (20). Transfected 293T cells were washed with phosphate-buffered saline (PBS) after incubation at 37°C, fixed for 10 min with 4% formaldehyde–PBS, and reacted with a mixture of anti-HPIV3 HN monoclonal antibodies supplied by Judy Beeler from the World Health Organization repository or anti-NDV AV HN monoclonal antibodies supplied by Ronald Iorio (in PBS supplemented with 0.05% sodium azide and 3% bovine serum albumin). The cells were left at room temperature for 30 min and then washed three times with PBS. Horseradish peroxidase-conjugated anti-mouse immunoglobulin G (Bio-Rad) was then added to the cells in the PBS–1% bovine serum albumin (1:10,000 dilution), which were then incubated for 30 min at room temperature. The cells were washed three times with PBS before incubation with TMB (3,3′,5,5′ tetramethylbenzidine) substrate (Pierce) as per the manufacturer's protocol. Absorbance measurements were taken at 450 nm with an ELISA reader (EL 312; Bio-Tek Instruments, Winooski, VT).

HAD assays. Hemadsorption (HAD) was performed and quantified as previously described (22). Following aspiration of the medium from transfected 293T cell monolayers in 24- or 48-well Biocoat plates (Becton Dickson Labware, Bedford, MA), the medium was replaced with 300 or 150 μl of 1% red blood cells (RBCs) in serum-free, CO_2-independent medium (pH 7.3) and placed at 4°C for 30 min. The wells were then washed three times with 300 or 150 μl cold CO_2-independent medium (catalog number 18045-088; Gibco, Gaithersburg, MD). The bound RBCs were lysed with 200 μl RBC lysis solution (0.145 M NH_4Cl, 17 mM Tris HCl), and the absorbance was read at 540 nm on the Bio-Tek ELISA reader.

Assay of neuraminidase activity. Neuraminidase assays were performed in transiently transfected 293T cell monolayers as previously described (17).

Partial removal of sialic acid receptors from RBCs. Partial receptor depletion of red blood cells was achieved by treatment of 2 ml of a 10% RBC solution in serum-free medium for 2 h at 37°C with 0 to 50 mU of *Clostridium perfringens* neuraminidase (type X from *C. perfringens*, catalog number N-2876; Sigma Scientific, St. Louis, MO) as described previously (20). Neuraminidase was then removed by washing the RBCs three times with serum-free medium. Each set of RBCs was then resuspended in serum-free, CO_2-independent medium to make final RBC stocks of 2% RBCs.

Use of receptor-depleted RBCs to assess HN receptor-binding avidity. RBCs partially depleted of their surface sialic acid receptors (described above) were used to determine the relative receptor-binding avidities of variant HN molecules as described previously (20). In each experiment, all the RBCs were from the same preparation of depleted stocks (as described above). The RBCs were overlaid onto 48-well plates of 293T cell monolayers transiently transfected 48 h prior with WT or variant HN expressed as described above. The plates were placed at 4°C for 30 min to allow RBC binding. The cell monolayers were then washed at 4°C with cold CO_2-independent medium to remove unbound RBCs, the bound RBCs were lysed (0.145 M NH_4Cl, 17 mM Tris HCl), and the absorbance was read at 540 nm on the Bio-Tek ELISA reader. Results are presented as the percent retention of RBCs relative to control (undepleted RBCs) versus the degree of depletion expressed as milliunits of bacterial neuraminidase.

Molecular models. Molecular models for the ligand-bound active sites were built from available crystallographic structures: NDV HN bound with DANA (Protein Data Bank [pdb] code [8] 1e8v) in site I of NDV, and NDV HN bound with DANA in site I, thiosialoside in site II of chain A, and sialic acid in site II of chain B (1usr) (28) in site II of NDV. Ligand molecules were superimposed over these substrate references by matching chemical moieties in three dimensions. Modeling, visualization, and optimization were performed with the Sybyl suite of programs (Tripos, Inc., St. Louis, MO). The regions around the active sites (6-Å "hot" radius) were relaxed with a molecular force field energy mini-

mization to an energy gradient of 0.005 kcal mol^{-1} $Å^{-1}$ using standard parameters and procedures with the exception that the distance-dependent dielectric was changed to 4 because of the open nature and solvent accessibility of the active sites.

Hydropathic scoring. The relative energies of the bound ligands in the molecular models were evaluated with the HINT (Hydropathic INTeractions; Tripos, Inc., St. Louis, MO) program (14, 16, 27). This program uses a unique non-Newtonian force field derived from experimental measurements of solvent partitioning to calculate free-energy scores that can be readily converted to binding free energies (4, 7, 10, 11). In this work, HINT 3.10S, which includes a number of local modifications (15, 26), was used to calculate binding scores. The hydrogen treatment option was set to "essential," which explicitly considers all polar hydrogens but incorporates nonpolar hydrogens as part of their heavy atom (i.e., the hydrogens of a methyl are subsumed into the carbon united "CH_3" atom). In addition, the solvent-accessible surface areas for protein backbone nitrogens were corrected with the "+30" option. HINT scores were converted to free energies of binding using an equation derived earlier for DANA and analogues bound to neuramindase (10), $\Delta G = -0.0020\ H_{TOTAL} + 4.052$, where H_{TOTAL} is the total HINT score for the protein-ligand interaction.

RESULTS

Resistance of the binding properties of NDV-AV HN to zanamivir or DANA. The zanamivir resistance of the attenuated strain of NDV, B1 Hitchner (24), was also exhibited by the HN of the pathogenic NDV-AV strain. As shown in Fig. 3, the NDV-AV HN is highly resistant to the binding-inhibitory effects of zanamivir or DANA. At a concentration of 1 mM zanamivir, HAD is inhibited by 25 to 30%, but a further increase in the concentration of zanamivir causes no additional inhibition. Residual receptor binding (approximately 70%) could not be completely inhibited even at the highest concentrations of zanamivir. Similar results are shown (Fig. 3) for DANA. The neuraminidase activity, however, as for the NDV B1 HN, was completely inhibited by 5 mM zanamivir or DANA. Neuraminidase inhibition assays were performed with 293T cells expressing NDV HN, using a 10 mM concentration of the substrate MUNANA. In each instance, HN expression levels were determined and the results were normalized as described previously (24). The NDV AV HN was inhibited about 94% in the presence of either 5 mM zanamivir or 5 mM DANA. The NDV AV HN neuraminidase activities were 22.3 ± 3.6 nmol/min for the control, 1.5 ± 0.8 nmol/min in the presence of 5 mM zanamivir, and 1.4 ± 0.2 nmol/min in the presence of 5 mM DANA. Given the comparable effectiveness of zanamivir and DANA on NDV-B1 Hitchner HN (24), and since similar inhibition of both neuraminidase and receptor binding was obtained for NDV-AV HN with zanamivir and DANA in this study, these studies were continued using zanamivir. Also, because the inhibitor-resistance pattern of HN of the pathogenic NDV-AV strain was similar to that of the attenuated B1 strain HN (24), the present studies used the NDV-AV HN.

NDV HN receptor-binding site I is zanamivir sensitive; site II mediates receptor binding when site I is occupied by zanamivir. One interpretation of the data shown in Fig. 3 is that the partial inhibition of receptor binding is due to the blocking of site I while the approximately 70% residual binding is mediated by the zanamivir-resistant site II. To test this hypothesis, a strategy was developed to separate the functions of the two sites. In these studies, target cells (RBCs) were bound to HN-expressing cells at 4°C in the presence or absence of zanamivir, and after transfer to 37°C, the release of these RBCs was measured with and without added zanamivir. Receptor cleavage and target cell release from HN of NDV is mediated by site I's neuraminidase activity, and zanamivir inhibits NDV neuraminidase (24). The efficiency with which HN dissociates from the receptor, and releases prebound RBCs, depends simultaneously on neuraminidase activity and binding, since a change in either property will affect receptor dissociation (20, 23). Thus, if binding at 4°C in the presence of zanamivir (which occupies site I) was in fact attributable to site II of NDV HN alone, then zanamivir added at the time of transfer to 37°C should inhibit RBC release at 37°C by blocking the neuraminidase activity of site I. If, on the other hand, site I was involved in receptor binding at 4°C in the absence of zanamivir, then zanamivir added at 37°C would compete for this binding and promote receptor dissociation and RBC release (as shown previously for HPIV3 [12, 20]).

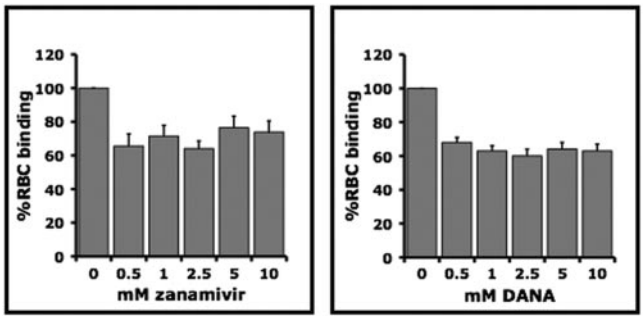

FIG. 3. Sensitivity of NDV HN receptor-binding activity to zanamivir or DANA. Cell monolayers transiently expressing NDV AV HN were assayed using HAD (at 4°C) as described in Materials and Methods. The binding (*y* axis) at the indicated concentrations of zanamivir or DANA (*x* axis) is expressed as the percent RBC binding obtained in the absence of an inhibitor. The results are means of results on triplicate wells from representative experiments, with bars denoting standard deviations.

Figure 4A shows that the first hypothesis mentioned above is correct; zanamivir added to NDV HN-expressing cells at the time of transfer to 37°C inhibits HN-receptor dissociation and RBC release. In the aliquots without zanamivir, RBC release continued throughout the 3-h incubation at 37°C. If site I of NDV HN (and not, as proposed, site II) were responsible for receptor binding at 4°C in the presence of zanamivir, then zanamivir, an inhibitor of this site's attachment function, would compete with the RBCs for binding and promote their release. This is clearly not the case. Thus, the results indicate that zanamivir—while allowing target cell receptor binding mediated by site II—prevented target cell release at 37°C by blocking the neuraminidase activity of site I.

HPIV3 T193I HN represents an ideal control for this experiment, because the pocket containing residue 193 is responsible for receptor binding at 4°C in the presence of zanamivir and zanamivir simultaneously inhibits HPIV3 HN′s receptor binding and its neuraminidase activity (20, 23). The experiment shown in Fig. 4B was carried out under identical conditions to the NDV experiment shown in Fig. 4A but by using cells expressing HPIV3 T193I HN. For these cells, zanamivir enhanced the rate of receptor dissociation and therefore the release of RBCs. This observation highlights the difference between the behavior of HPIV3 and NDV HN under the same conditions: for NDV, the second site, which is zanamivir resis-

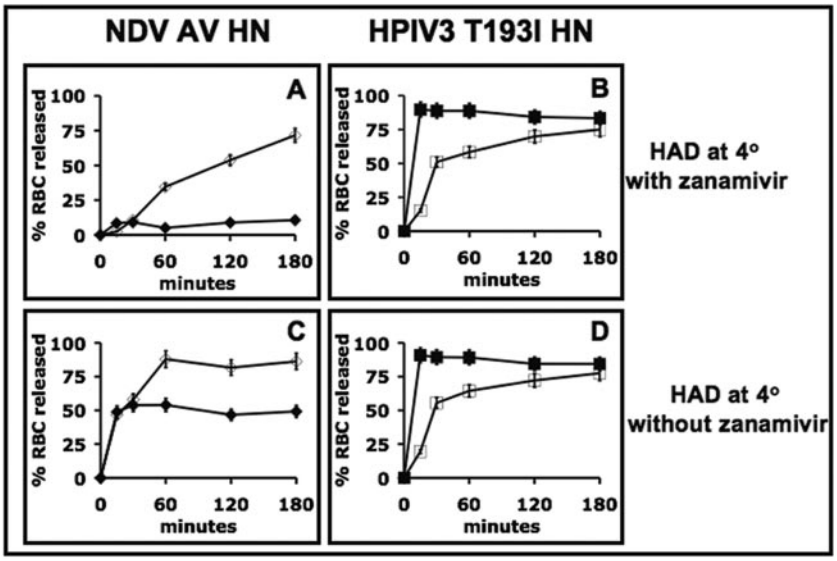

FIG. 4. Release of target RBCs that were prebound to NDV HN- or to HPIV3 T193I HN-expressing cells in the presence (A and B) or absence (C and D) of zanamivir. For the experiments in panels A and B, HAD at 4°C was carried out on cells expressing NDV HN (diamonds) or HPIV3-T193I-HN (squares) in the presence of 10 mM zanamivir. The cells were then rinsed free of zanamivir and transferred to 37°C, and the release of RBCs was determined in the absence (open symbols) or presence (closed symbols) of 10 mM zanamivir. The amounts of RBCs released at the indicated times (*x* axis) are expressed as the percent RBCs that were bound at the end of the HAD period (i.e., at time point zero). Panels C and D show the results of experiments identical to those above except that zanamivir was not present during the 4°C HAD period. The results are means of results on triplicate wells from representative experiments, with bars denoting standard deviations.

tant, can carry out binding at the same time that the first site, the zanamivir-sensitive site, is inhibited.

If zanamivir's occupation of NDV HN site I during the 4°C HAD means that binding must be mediated by site II alone, then the results of RBC release experiments should be different if the HAD is performed without zanamivir. NDV HN site I would mediate binding in the absence of zanamivir, and zanamivir should compete with the RBCs for site I binding, thus promoting release. Figure 4C shows the release of RBCs that had been prebound to NDV HN-expressing cells in the absence of zanamivir. As a control, the identical experiment using HPIV3 T193I HN was performed, since zanamivir is expected to enhance HN-receptor dissociation under either HAD condition for HPIV3 T193I HN (i.e., whether or not zanamivir is present during the 4°C incubation). Zanamivir indeed enhanced the release of RBCs from HPIV3 HN-expressing cells (Fig. 4D), similar to the results in Fig. 4B where zanamivir was present during HAD.

For NDV HN, however, Fig. 4C shows that without zanamivir present during the HAD period, RBC release is no longer inhibited by zanamivir addition at 37°C. The simplest explanation for these findings is that without zanamivir present, NDV HN site I can mediate binding. Note that in Fig. 4C, the RBC release from NDV HN-expressing cells in the presence of zanamivir is initially rapid but soon slows and 50% of the RBCs remain bound. One possible explanation for this observation is that some of the RBCs that are released from site I by zanamivir competition later bind to site II. Once bound to site II, these RBCs remain attached because zanamivir blocks only the site I neuraminidase activity but cannot inhibit site II; it does not compete with receptors on the RBCs for site II.

Zanamivir increases the receptor-binding avidity of NDV HN. We have previously developed a quantitative receptor avidity assay (20, 25) and shown that NDV HN has low avidity for receptors on RBCs (either human or avian) compared to the HPIV3 HNs (24). This receptor avidity assay was then used to specifically measure the avidity of NDV HN site II and compare it to the avidity of site I. In this assay, receptor-depleted RBCs are bound to HN-expressing cells in a quantitative HAD (the higher the avidity, the greater receptor depletion is required to reduce binding). At 4°C, neither NDV nor HPIV3 neuraminidases are active and therefore cannot contribute to RBC release. Based on these results, in the presence of zanamivir, HAD should result from site II binding only, allowing its avidity to be assessed.

Figure 5 shows the results of an experiment comparing the binding avidity of NDV HN in the presence or absence of zanamivir. For comparison of HPIV3 with NDV, the partially zanamivir-resistant T193I HN was again used. While the T193I HN binds receptor in the presence of zanamivir, its partial zanamivir sensitivity can be revealed by using partially receptor-depleted RBCs in the binding assay (23). Figure 5A shows that HAD performed on NDV HN-expressing cells without zanamivir declines rapidly and reaches 50% binding at a depletion level of 10 mU. However, in the presence of zanamivir, the decline is more gradual and reaches 50% binding at a depletion level of 15 mU, indicating that receptor avidity of NDV HN is increased in the presence of zanamivir. In clear contrast to this surprising finding for NDV, Fig. 5B confirms that for HPIV3 T193I HN, HAD declines more rapidly in the presence of zanamivir.

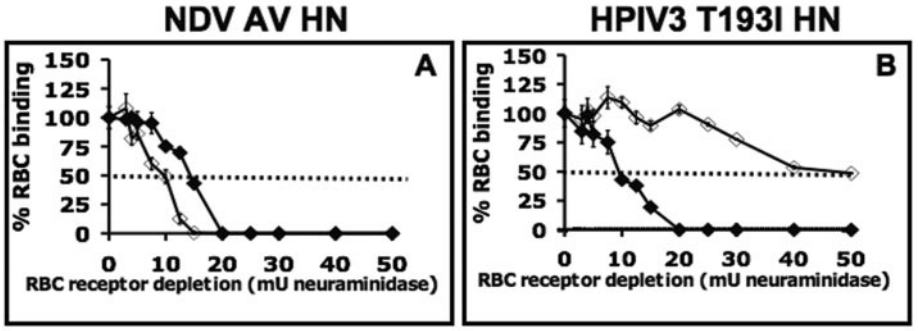

FIG. 5. Effects of zanamivir on receptor binding by NDV HN and HPIV3 T193I HN. A panel of RBCs with different degrees of receptor depletion (prepared as described in Materials and Methods) was used to quantify HAD on cell monolayers expressing NDV HN (A) or HPIV3 T193I HN (B) in the absence (open symbols) or presence (closed symbols) of 10 mM zanamivir at 4°C. At 4°C, neither NDV nor HPIV3 neuraminidases were active. The extent of binding of each depleted RBC preparation (*y* axis) is expressed as a percentage of that of the control (i.e., of the amount of untreated, nondepleted RBCs bound to cells expressing the corresponding HN). The points are means of results on triplicate monolayers from three representative experiments, with bars denoting standard deviations.

The antagonistic effect of zanamivir and sialyllactose on NDV HN binding demonstrates that binding site II is activated by occupation of site I. The finding (Fig. 5) that the NDV HN receptor-binding avidity is increased in the presence of zanamivir was unexpected. This result, together with the fact (Fig. 4) that site II mediates receptor binding in the presence of zanamivir, led to two possible hypotheses: (i) binding site I mediates binding in the absence of zanamivir, and site II becomes active only when site I is occupied, or (ii) site II is the constitutive binding site, and its binding is enhanced by zanamivir; in this scenario, the only function of site I is its neuraminidase activity.

Testing these hypotheses required an inhibitor that would completely abolish binding by NDV HN. We determined that 2,3-sialyllactose, a naturally occurring substrate of the HN neuraminidase, does just that. 2,3-Sialyllactose mimics the cellular receptor moiety recognized by avian pathogens including NDV. If site II were the constitutive binding site, then the effects of 2,3-sialyllactose and zanamivir would be additive: adding zanamivir would increase the avidity of site II, and 2,3-sialyllactose would block site II more effectively. If, however, site II becomes active only when site I is occupied by zanamivir, then 2,3-sialyllactose and zanamivir should compete for site I and have antagonistic effects; once zanamivir inhabits site I, binding would be activated at site II and 2,3-sialyllactose would not be able to inhibit binding.

The extent of binding inhibition by different concentrations of 2,3-sialyllactose was determined at 4°C in the presence or absence of zanamivir. The results in Fig. 6 show that NDV HN receptor binding was completely inhibited at a concentration of 2.0 mM 2,3-sialyllactose. When 2,6-sialyllactose was used, there was no inhibition (data not shown), indicating that binding is specific for the 2,3 linkage, as expected. As can be seen in Fig. 6, the effects of 2,3-sialyllactose and zanamivir are antagonistic. Addition of zanamivir decreased the inhibitory effect of 2,3-sialyllactose dramatically. This result indicates that 2,3-sialyllactose in the absence of zanamivir binds site I and cannot bind to site II. Also, when site II becomes active because site I is occupied by zanamivir, 2,3-sialyllactose fails to completely inhibit RBC binding.

The fact that 2,3-sialyllactose provides 100% inhibition of binding in the absence of zanamivir indicates that, unless zanamivir is present, site II exerts no binding activity and the NDV HN receptor-binding avidity is entirely attributable to site I. When zanamivir is present, however, receptor binding is mediated entirely by site II, because site II is apparently functional only when site I is occupied by zanamivir. Furthermore, 2,3-sialyllactose can completely inhibit binding only because, unlike zanamivir, it does not appear to activate site II.

As an alternative explanation for these results, we asked whether increased avidity in the presence of zanamivir in Fig. 5A could be attributed to zanamivir's inhibition of neuraminidase even at 4°C—a temperature where neuraminidase is not expected to be active—rather than to activation of site II. However, if neuraminidase were in fact active at 4°C, this effect would have also been seen in Fig. 6; instead of the antagonistic effect of zanamivir on 2,3-sialyllactose seen in Fig. 6, a synergistic effect would have been observed. Since 2,3-sialyllactose is a substrate for neuraminidase activity, block-

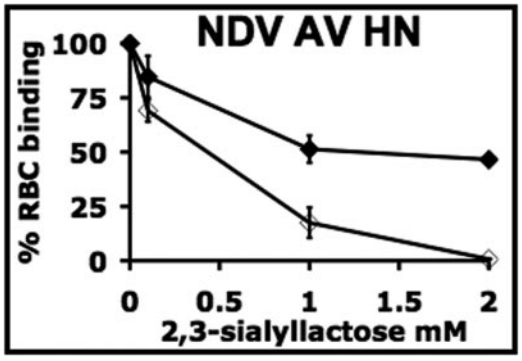

FIG. 6. Effect of zanamivir on sialyllactose inhibition of NDV HN receptor binding. Quantitative HAD on cells expressing NDV HN was carried out in the presence of increasing concentrations of 2,3-sialyllactose and in the absence (open symbols) or presence (closed symbols) of 10 mM zanamivir at 4°C. At 4°C, neither NDV nor HPIV3 neuraminidases were active. The RBC binding (*y* axis) at the indicated concentrations of sialyllactose (*x* axis) is expressed as a percentage of the binding obtained in the absence of sialyllactose. Points are means of results on triplicate monolayers from three representative experiments, with bars denoting standard deviations.

ing neuraminidase would have prevented the cleavage of 2,3-siallyllactose. The antagonistic effect seen in Fig. 6 rules out this possibility.

The unexpected findings shown in Fig. 5, that NDV HN receptor binding is increased by zanamivir, can now be explained. In the presence of zanamivir, the observed binding (Fig. 5A) is attributable to site II, while in the absence of zanamivir, the observed binding is mediated by site I. We also considered the possibility that instead, siallylactose binds site I and activates site II but then blocks both sites I and II. However, if this were true, then siallylactose and zanamivir would not be antagonistic in the Fig. 6 experiment. Taking Fig. 5 and 6 together, the results reveal the relative receptor-binding potentials of sites I and II. Site II can bind cellular receptors more strongly than site I, as shown by the greater binding in Fig. 5A in the presence of zanamivir. This binding potential is revealed only in the presence of zanamivir. The molecular modeling results, below, will further illuminate this result, and this topic will be explored further in the Discussion.

Molecular modeling of the NDV HN active sites. It was of interest to test whether the varying abilities of zanamivir, DANA, BCX 2798, and sialyllactose to activate site II might be explained by computational examinations of the strength of interaction between these small molecules and the active sites. Note that while one site I is fully contained within each NDV HN molecule, site II is found at interfaces when dimers or higher multimers are formed, such that there is one site II for each NDV HN molecule (and for each site I). These computational studies were performed using the two crystal structures of NDV HN dimers (8, 28), which have these sites occupied by DANA (site I), thiosialoside (site II chain A), and sialic acid (site II chain B) as templates for modeling the bound conformation of DANA, zanamivir, 2,3-sialyllactose, 2,6-sialyllactose, and BCX 2798 (2) at these sites.

Both thiosialoside and sialic acid bind to site II through the sialic acid group that each possesses. Site II of chain A (Fig. 2) shows some differences from site II of chain B, e.g., the side chain of Arg516 is oriented toward the carboxylate group of the ligand and forms hydrogen bonds with the carboxylate oxygen atoms of the sialic group in chain A, while this Arg side chain has been reported as being turned away from the sialic group at the chain B site II. To investigate this further, the computational experiments were performed on site II both from chain A and from chain B.

Two modeling issues with this data set need clarification. First, the azido group of BCX 2798 is particularly difficult to model with most force fields. In the Tripos force field used in this study, the only reasonable parameterization was $-N.2 = N.1 = N.2$, where N.2 refers to an sp^2 nitrogen and N.1 refers to an sp hydrogen. In addition, the central nitrogen has a formal +1 charge, while the terminal nitrogen has a formal −1 charge. However, this parameterization was problematical in the structural optimizations of HN complexes with BCX 2798. Thus, the azido group, once built, was treated as an aggregate and was withheld from further optimization to maintain its linear structure. Similarly, the HINT model has poorly developed hydropathic parameters for azido; azido is also a "missing fragment" in CLOGP (Biobyte, Claremont, CA), a program generally accepted as the standard for estimation of log P for 1-octanol-water partitioning.

TABLE 1. Binding energy for the interactions of the small molecules with the two NDV HN active sites relative to that of DANA bound at the first HN active site (site I)

Active site (crystal reference)	Ligand	HINT score	ΔΔG (kcal mol^{-1})
Site I (1e8v)	DANA (crystal)[a]	3,009	0.00
	DANA (minimized)[b]	2,632	0.75
	2,3-Sialyllactose[c]	2,828	0.36
	2,6-Sialyllactose[c]	1,645	2.73
	Zanamivir[d]	3,733	−1.45
	Zanamivir (1v3e)[e]	3,480	−0.94
	BCX 2798[d]	3,564	−1.11
Site II chain A (1usr)	Thiosialoside[a]	709	4.60
	2,3-Sialyllactose[c]	1,750	2.52
	2,6-Sialyllactose[c]	1,534	2.95
	Zanamivir[c]	1,051	3.92
	BCX 2798[c]	−1,662	9.34
	DANA[c]	−99	6.22
Site II chain B (1usr)	Sialic acid[a]	200	6.42
	2,3-Sialyllactose[c]	109	5.80
	2,6-Sialyllactose[c]	62	5.89
	Zanamivir[c]	−717	7.45
	BCX 2798[c]	−1,313	8.64
	DANA[c]	−153	6.32

[a] Ligand experimentally determined in crystal complex; only hydrogens were minimized.
[b] DANA and 6-Å region surrounding DANA were structure optimized.
[c] Ligand structures built and optimized external to site, superimposed on crystallographic ligand, followed by 6-Å region site optimization.
[d] Ligand structure built as modifications of crystallographic ligand at site (see text for details).
[e] Zanamivir taken from crystal structure of HN HPIV3 (pdb 1v3e) (17) and superimposed to DANA into 1e8v active site.

The second issue concerns the modeling of the noncrystallographic ligands in the two active sites. In all cases, the crystallographic ligand was used as the starting point (DANA in site I, thiosialoside in site IIA, and sialic acid in site IIB as described in Materials and Methods). New ligands were then, generally, built and optimized external to the active site and then superimposed to the crystallographic ligand, followed by a further in situ optimization. For site I DANA, the results are reported here for both the crystallographic configuration and for one in which DANA was optimized in the site with the same methods as for the other ligands. The rough estimate of reproducibility of the techniques thus obtained was about ± 0.75 kcal mol^{-1}. Zanamivir was also modeled in two ways: first, as described above, and second, by placing zanamivir from pdb structure 1v3e (HPIV3 HN) followed by minimization. The reproducibility here was about ± 0.50 kcal mol^{-1}.

For site I of NDV HN, the computational study (Table 1) indicated that zanamivir (I) and BCX 2798 (VII) have similar binding free energies and both bind to NDV HN more strongly than DANA (II). All results in Table 1 are reported as differences from the calculated binding free energy of DANA, the ligand found in site I of the crystal structure. Zanamivir bound to HN about 1 kcal mol^{-1} more strongly than DANA, which would roughly correspond to about 1 order of magnitude difference in the binding constant. The strength of interaction for 2,3-sialyllactose was comparable to that for DANA, while 2,6-sialyllactose interacted rather weakly with site I of NDV HN,

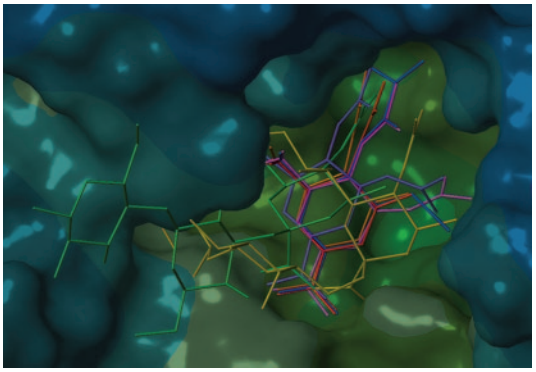

FIG. 7. Ligands bound and superimposed to NDV HN site I. The five ligands modeled into NDV HN site I are shown superimposed. DANA is represented in both its crystallographic configuration (red-orange) and its optimized configuration (orange). Zanamivir is shown in the two modeled configurations: built in situ from the crystallographic ligand DANA (purple) and as taken from the crystal structure of HPIV3HN (magenta). 2,3-Sialyllactose, 2,6-sialyllactose, and BCX 2798 are shown in green, yellow, and blue, respectively. The lipophilic surface contour of the protein around the active site (blue, polar; brown, lipophilic) was created with MOLCAD (Tripos, Inc., St. Louis, MO).

having a $\Delta\Delta G$ (relative to DANA) of about 2.7 kcal mol^{-1}, a binding constant which was more than 2 orders of magnitude weaker. Figure 7 shows the five site I ligands superimposed at the site. As modeled, all of these present the sialic acid moiety to HN in a similar fashion.

Evaluation of both chain A and chain B site II binding of NDV HN (Table 1) shows that all the small molecules considered bind either weakly or not at all. The results show different binding values for the interactions of the small molecules with site II from chain A and chain B: the molecules interacting with the site on chain B show significantly weaker interactions, likely due to the different orientations of Arg516 in the two chains. In addition, two crystallographic observations are significant. First, the occupancy factor, a parameter that defines the partial residency of a given site by a particular atom, is less than 1 (0.67) for the sialic acid bound to the second site of chain B. Second, the "B" factor, a crystallographic measure of disorder and thermal motion, is about twice as large for the atoms in the Arg516 residue of chain B as that for atoms in Arg516 of chain A. These two observations are further evidence that site II may be transient compared to site I, at least when DANA is occupying site I.

DISCUSSION

We have shown that while both zanamivir and 2,3-sialyllactose inhibit binding at receptor-binding site I of NDV HN, only zanamivir's binding leads to the activation of binding site II. Site II receptor binding arises from interaction with sialic acid-containing receptors, as evidenced by the negative effect of neuraminidase treatment on NDV HN site II receptor binding (Fig. 5A). In addition, while zanamivir and 2,3-sialyllactose both interact with NDV HN site I, neither appears to interact with site II. It was especially surprising that 2,3-sialyllactose, a receptor mimic, did not interact with binding site II on NDV HN, as shown experimentally by its failure to inhibit binding in the presence of zanamivir. In the discussion below, we propose a mechanism that explains these observations and describe some of the implications of this mechanism.

Proposed mechanisms for regulation of receptor-binding site I on NDV HN by site II. The second binding site on NDV HN, revealed by cocrystallization with thiosialoside (28), was found to be located on the dimer interface of the molecule and made up of hydrophobic residues from both monomers. The involvement of the Arg516 side chain in the interaction with sialic acid suggested that Arg516, a residue that is strongly conserved among NDV isolates, is important for the function of site II (28). Mutations at this residue (R516A or R516S) result in HNs that, when coexpressed with F, are less efficient in fusion promotion (3), suggesting that site II may play a role in the HN fusion promotion function during viral entry (3, 28). However, these HNs mutated at site II (R516A or R516S) were found to bind RBCs similarly to WT HN in hemagglutination assays, a finding previously interpreted to mean that site II did not contribute to receptor-binding activity (3). The present finding that the NDV HN receptor-binding avidity is considerably increased with activation of site II by zanamivir occupation of site I suggests that site II may in fact contribute to receptor binding at specific times in the viral entry process.

The finding that site II requires activation could explain why HNs mutated at residues in and around site II—while defective in fusion promotion—were observed by Corey et al. to bind receptor normally at 4°C. The observed binding in that experiment occurred at site I, but site II, because of its mutations, remained inactive during the fusion assay at 37°C. Therefore, binding and consequent fusion promotion were impaired (6). Thus, at 4°C, binding occurred via site I alone because the binding of the site II mutants was similar to the WT, but site I alone was not adequate for efficient binding at 37°C. These data are consistent with the suggestion that site II is activated by occupation of site I; in the case of a mutated site II, activation does not result in the binding that is essential for fusion promotion at 37°C.

The possibility of a conformational change in NDV HN upon binding to a receptor-mimic was suggested by studies in which binding to free gangliosides led to exposure of hydrophobic sites on HN (9). Structural studies also support this notion, since the second binding site was identified only in the structure that was solved with the first binding site occupied (28). These crystallographic structures, however, indicate somewhat poorly developed site II geometries with relatively high structural uncertainty and significant disorder. The modeling results, suggesting that BCX 2798 has a binding free energy similar to that of zanamivir and binds NDV HN more strongly than DANA, are consistent with the hypothesis that this molecule, upon binding to site I, activates site II. If so, this would explain why BCX 2798 effectively inhibits HPIV3 HN binding but does not inhibit NDV HN binding unless site II is mutated (R516A) (3). Like zanamivir, this molecule binds effectively enough to site I such that it activates site II but does not inhibit site II.

Figure 8 summarizes these observations for NDV HN. Figure 8A illustrates that NDV HN site I is active and available for target cell receptor binding while site II is inactive and unable to bind target cell receptors. In Fig. 8B, a 2,3-sialyllactose molecule is bound in site I, thus blocking site I from RBC binding; in addition, 2,3-sialyllactose is unable to activate site

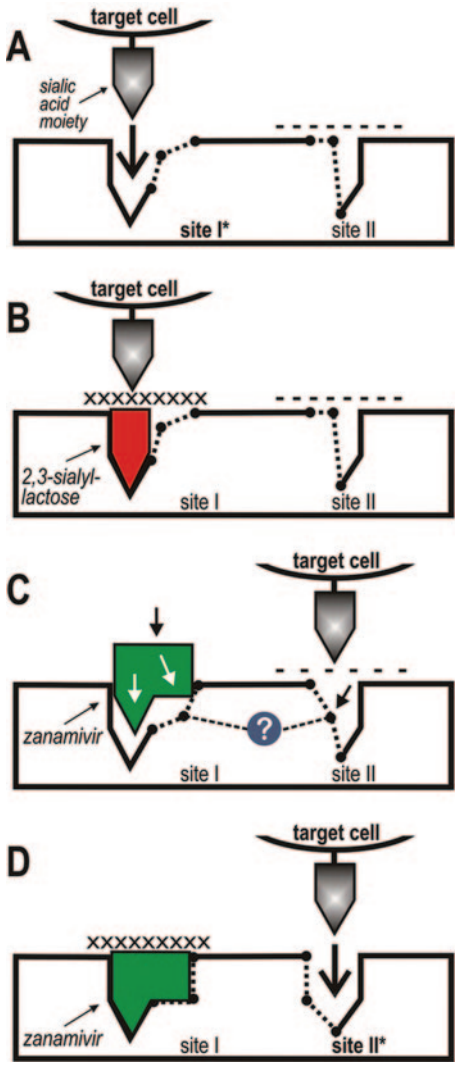

FIG. 8. Mechanism of target cell receptor binding to NDV HN′s binding sites I and II and the response to 2,3-sialyllactose or zanamivir. (A) Site I is active and subject to target cell receptor binding in the absence of ligand, while site II is inactive. (B) 2,3-Sialyllactose blocks site I but fails to activate site II. (C) A structural change that activates site II is induced (through an unknown mechanism) upon zanamivir binding to site I. (D) Site II is active and subject to target cell receptor binding in the presence of zanamivir, while site I is blocked.

II. The entrance of zanamivir is illustrated in Fig. 8C. Although the precise mechanism is unknown at this time, there may be an interaction between sites I and II such that the occupation of site I by zanamivir induces an activating structural change in site II. With zanamivir fully bound at site I (Fig. 8D), site II becomes active and available for target cell receptor binding.

Implications of the proposed mechanism for paramyxovirus entry. The second receptor-binding site on NDV HN, located at the dimer interface, becomes activated when the globular head-binding site is occupied by zanamivir, a transition state analog of sialic acid, but does not become activated by the receptor analog 2,3-sialyllactose. Two possible explanations may be proposed for these findings. The lower binding avidity of 2,3-sialyllactose for site I, suggested by molecular modeling and calculated free energies of binding (Table 1), may be below the threshold required for activation of site II. A more interesting possibility is that generation of a transition state compound in active site I during receptor interaction leads to the activation of site II. Such a reaction intermediate, which would resemble zanamivir rather than 2,3-sialyllactose, may activate site II under physiological conditions. In this case, one could envision that after initial binding of NDV-HN via its bifunctional site I to a new cell and initiation of neuraminidase cleavage of receptor moieties, the second site, which binds more avidly but lacks neuraminidase, becomes activated. The timing would be propitious; at the time of viral entry, avid binding and fusion with the target cell are needed.

The higher receptor avidity of NDV HN, when zanamivir is occupying site I (Fig. 5), reveals that site II has greater potential binding avidity than site I, and this difference in binding capacity of the two sites means that the binding avidity of NDV HN could be regulated by controlling the activation of site II. We have previously shown that each of the three discrete properties of HN, receptor binding, neuraminidase activity, and F triggering, can independently affect the ability of HN to activate F, thus mediating fusion. For example, higher neuraminidase activity decreases the period of HN-receptor contact that is essential for F triggering, thus decreasing fusion; however, higher receptor avidity can compensate for this effect. The ratio of neuraminidase activity to binding avidity is higher for NDV than for HPIV3. While neuraminidase activity is advantageous during budding and release of new NDV virions to ensure that no virions remain bound to cell membrane receptors, it could be a disadvantage during binding and entry. Site I of NDV HN alone, with its high neuraminidase-to-receptor avidity ratio, would not assure effective entry. Site II activation may explain how NDV HN achieves adequate binding for fusion promotion; an activated site II, with its higher receptor-binding avidity and no neuraminidase activity, could carry out these functions. One may speculate that NDV has evolved a mechanism whereby site II is activated upon attachment of site I to a target cell but is shut off at the end of the budding process. This strategy would facilitate viral entry as well as the release of progeny virions by the neuraminidase activity of site I.

It should be noted that the molecular modeling results of Table 1 appear to indicate that site I has greater potential binding avidity than site II. This is a consequence of several factors related to the structural differences between the two types of sites. Most importantly, site II is less occluded that site I, thus having fewer interactions with the ligands. As a result, more of the ligands' interactions at site II will be with water, which were not included in this molecular modeling study. However, this openness of site II may also make it easier for target cells to approach this site with their sialic acid moieties.

Apparently, to effectively inhibit NDV HN binding, a molecule needs to block site I as does 2,3-sialyllactose, without activating site II (or to block both sites). This provides a design strategy for the development of new inhibitors, and understanding how some receptor analog molecules activate site II while other, seemingly quite similar, molecules do not, is a critical issue. Of obvious value would be additional experimental structural data for NDV HN-ligand complexes. The mechanism by which zanamivir in site I activates binding site II is of

interest, since it would provide insight into the roles of distinct regions of NDV HN in the multiple functions of this molecule. Understanding how this activation occurs may help determine how the two binding sites are regulated under the physiological conditions of viral infection.

ACKNOWLEDGMENTS

This work was supported by Public Health Service grants AI 31971 to A.M. and GM 71894 to G.E.K. from the National Institutes of Health.

We thank Judy Beeler and Ron Iorio for providing needed reagents, Joshua Zimmerberg for helpful discussions, Lynne M. Doctor for helpful discussions and thoughtful editing of the manuscript, and Gerald M. Loughlin for the research environment.

REFERENCES

1. **Alymova, I. V., A. Portner, T. Takimoto, K. L. Boyd, Y. S. Babu, and J. A. McCullers.** 2005. The novel parainfluenza virus hemagglutinin-neuraminidase inhibitor BCX 2798 prevents lethal synergism between a paramyxovirus and *Streptococcus pneumoniae*. Antimicrob. Agents Chemother. **49:**398–405.
2. **Alymova, I. V., G. Taylor, T. Takimoto, T. H. Lin, P. Chand, Y. S. Babu, C. Li, X. Xiong, and A. Portner.** 2004. Efficacy of novel hemagglutinin-neuraminidase inhibitors BCX 2798 and BCX 2855 against human parainfluenza viruses in vitro and in vivo. Antimicrob. Agents Chemother. **48:**1495–1502.
3. **Bousse, T. L., G. Taylor, S. Krishnamurthy, A. Portner, S. K. Samal, and T. Takimoto.** 2004. Biological significance of the second receptor binding site of Newcastle disease virus hemagglutinin-neuraminidase protein. J. Virol. **78:** 13351–13355.
4. **Burnett, J. C., P. Botti, D. Abraham, and G. Kellogg.** 2001. Computationally accessible method for estimating free energy changes resulting from site-specific mutations of biomolecules: systematic model building and structural/hydropathic analysis of deoxy and oxy hemoglobins. Proteins **42:**355–377.
5. **Connaris, H., T. Takimoto, R. Russell, S. Crennell, I. Moustafa, A. Portner, and G. Taylor.** 2002. Probing the sialic acid binding site of the hemagglutinin-neuraminidase of Newcastle disease virus: identification of key amino acids involved in cell binding, catalysis, and fusion. J. Virol. **76:**1816–1824.
6. **Corey, E. A., A. M. Mirza, E. Levandowsky, and R. M. Iorio.** 2003. Fusion deficiency induced by mutations at the dimer interface in the Newcastle disease virus hemagglutinin-neuraminidase is due to a temperature-dependent defect in receptor binding. J. Virol. **77:**6913–6922.
7. **Cozzini, P., M. Fornabaio, A. Marabotti, D. J. Abraham, G. E. Kellogg, and A. Mozzarelli.** 2002. Simple, intuitive calculations of free energy of binding for protein-ligand complexes. 1. Models without explicit constrained water. J. Med. Chem. **45:**2469–2483.
8. **Crennell, S., T. Takimoto, A. Portner, and G. Taylor.** 2000. Crystal structure of the multifunctional paramyxovirus hemagglutinin-neuraminidase. Nat. Struct. Biol. **7:**1068–1074.
9. **Ferreira, L., E. Villar, and I. Munoz-Barroso.** 2004. Conformational changes of Newcastle disease virus envelope glycoproteins triggered by gangliosides. Eur. J. Biochem. **271:**581–588.
10. **Fornabaio, M., P. Cozzini, A. Mozzarelli, D. J. Abraham, and G. E. Kellogg.** 2003. Simple, intuitive calculations of free energy of binding for protein-ligand complexes. 2. Computational titration and pH effects in molecular models of neuraminidase-inhibitor complexes. J. Med. Chem. **46:**4487–4500.
11. **Fornabaio, M., F. Spyrakis, A. Mozzarelli, P. Cozzini, D. J. Abraham, and G. E. Kellogg.** 2004. Simple, intuitive calculations of free energy of binding for protein-ligand complexes. 3. The free energy contribution of structural water molecules in HIV-1 protease complexes. J. Med. Chem. **47:**4507–4516.
12. **Greengard, O., N. Poltoratskaia, E. Leikina, J. Zimmerberg, and A. Moscona.** 2000. The anti-influenza virus agent 4-GU-DANA (zanamivir) inhibits cell fusion mediated by human parainfluenza virus and influenza virus HA. J. Virol. **74:**11108–11114.
13. **Holzer, C., M. Von Itzstein, B. Jin, M. Pegg, W. Stewart, and W.-Y. Wu.** 1993. Inhibition of sialidases from viral, bacterial and mammalian sources by analogues of 2-deoxy-2,3-didehydro-*N*-acetylneuraminic acid modified at the C-4 position. Glycoconjugate J. **10:**40–44.
14. **Kellogg, G., and D. Abraham.** 2000. Hydrophobicity. Is $\log P_{o/w}$ more than the sum of its parts? Eur. J. Med. Chem. **35:**651–661.
15. **Kellogg, G., and D. Chen.** 2004. The importance of being exhaustive: optimization of bridging structural water molecules and water networks in models of biological systems. Chem. Biodiv. **1:**98–105.
16. **Kellogg, G. E., M. Fornabaio, F. Spyrakis, A. Lodola, P. Cozzini, A. Mozzarelli, and D. J. Abraham.** 2004. Getting it right: modeling of pH, solvent and "nearly" everything else in virtual screening of biological targets. J. Mol. Graph. Model. **22:**479–486.
17. **Lawrence, M. C., N. A. Borg, V. A. Streltsov, P. A. Pilling, V. C. Epa, J. N. Varghese, J. L. McKimm-Breschkin, and P. M. Colman.** 2004. Structure of the haemagglutinin-neuraminidase from human parainfluenza virus type III. J. Mol. Biol. **335:**1343–1357.
18. **Li, J., E. Quinlan, A. Mirza, and R. M. Iorio.** 2004. Mutated form of the Newcastle disease virus hemagglutinin-neuraminidase interacts with the homologous fusion protein despite deficiencies in both receptor recognition and fusion promotion. J. Virol. **78:**5299–5310.
19. **Moscona, A.** 2005. Entry of parainfluenza virus into cells as a target for interrupting childhood respiratory disease. J. Clin. Investig. **115:**1688–1698.
20. **Murrell, M., M. Porotto, T. Weber, O. Greengard, and A. Moscona.** 2003. Mutations in human parainfluenza virus type 3 HN causing increased receptor binding activity and resistance to the transition state sialic acid analog 4-GU-DANA (zanamivir). J. Virol. **77:**309–317.
21. **Plemper, R. K., A. S. Lakdawala, K. M. Gernert, J. P. Snyder, and R. W. Compans.** 2003. Structural features of paramyxovirus F protein required for fusion initiation. Biochemistry **42:**6645–6655.
22. **Porotto, M., O. Greengard, N. Poltoratskaia, M.-A. Horga, and A. Moscona.** 2001. Human parainfluenza virus type 3 HN-receptor interaction: effect of 4-guanidino-neu5Ac2en on a neuraminidase-deficient variant. J. Virol. **75:** 7481–7488.
23. **Porotto, M., M. Murrell, O. Greengard, L. Doctor, and A. Moscona.** 2005. Influence of the human parainfluenza virus 3 attachment protein's neuraminidase activity on its capacity to activate the fusion protein. J. Virol. **79:**2383–2392.
24. **Porotto, M., M. Murrell, O. Greengard, M. Lawrence, J. McKimm-Breschkin, and A. Moscona.** 2004. Inhibition of parainfluenza type 3 and Newcastle disease virus hemagglutinin-neuraminidase receptor binding: effect of receptor avidity and steric hindrance at the inhibitor binding sites. J. Virol. **78:** 13911–13919.
25. **Porotto, M., M. Murrell, O. Greengard, and A. Moscona.** 2003. Triggering of human parainfluenza virus 3 fusion protein (F) by the hemagglutinin-neuraminidase (HN): an HN mutation diminishes the rate of F activation and fusion. J. Virol. **77:**3647–3654.
26. **Spyrakis, F., M. Fornabaio, P. Cozzini, A. Mozzarelli, D. Abraham, and G. Kellogg.** 2004. Computational titration analysis of a multiprotic HIV-1 protease-ligand complex. J. Am. Chem. Soc. **126:**11764–11765.
27. **Wireko, F. C., G. E. Kellogg, and D. J. Abraham.** 1991. Allosteric modifiers of hemoglobin. 2. Crystallographically determined binding sites and hydrophobic binding/interaction analysis of novel hemoglobin oxygen effectors. J. Med. Chem. **34:**758–767.
28. **Zaitsev, V., M. von Itzstein, D. Groves, M. Kiefel, T. Takimoto, A. Portner, and G. Taylor.** 2004. Second sialic acid binding site in newcastle disease virus hemagglutinin-neuraminidase: implications for fusion. J. Virol. **78:**3733–3741.